U.S. Department of Transportation

Federal Railroad Administration

Load Environment of Rail Joint Bars—Phase II Joint Bar Service Environment and Fatigue Analysis

Office of Research and Development
Washington, DC 20590

DOT/FRA/ORD-14/22

Final Report
July 2014

NOTICE

This document is disseminated under the sponsorship of the Department of Transportation in the interest of information exchange. The United States Government assumes no liability for its contents or use thereof. Any opinions, findings and conclusions, or recommendations expressed in this material do not necessarily reflect the views or policies of the United States Government, nor does mention of trade names, commercial products, or organizations imply endorsement by the United States Government. The United States Government assumes no liability for the content or use of the material contained in this document.

NOTICE

The United States Government does not endorse products or manufacturers. Trade or manufacturers' names appear herein solely because they are considered essential to the objective of this report.

REPORT DOCUMENTATION PAGE

Form Approved
OMB No. 0704-0188

Public reporting burden for this collection of information is estimated to average 1 hour per response, including the time for reviewing instructions, searching existing data sources, gathering and maintaining the data needed, and completing and reviewing the collection of information. Send comments regarding this burden estimate or any other aspect of this collection of information, including suggestions for reducing this burden, to Washington Headquarters Services, Directorate for Information Operations and Reports, 1215 Jefferson Davis Highway, Suite 1204, Arlington, VA 22202-4302, and to the Office of Management and Budget, Paperwork Reduction Project (0704-0188), Washington, DC 20503.

1. AGENCY USE ONLY (Leave blank)	2. REPORT DATE	3. REPORT TYPE AND DATES COVERED
	July 2014	

4. TITLE AND SUBTITLE Load Environment of Rail Joint Bars – Phase II, Joint Bar Service Environment and Fatigue Analysis	5. FUNDING NUMBERS DTFR53-00-C-00012 Task Order 238
6. AUTHOR(S) and FRA COTR Muhammad Akhtar, Kevin Koch, Roy Wiley, and David Davis	
7. PERFORMING ORGANIZATION NAME(S) AND ADDRESS(ES) Transportation Technology Center, Inc. A subsidiary of Association of American Railroads PO Box 11130 Pueblo, CO 81001	8. PERFORMING ORGANIZATION REPORT NUMBER
9. SPONSORING/MONITORING AGENCY NAME(S) AND ADDRESS(ES) U.S. Department of Transportation Federal Railroad Administration Office of Research and Development Office of Railroad Policy and Development Washington, DC 20590	10. SPONSORING/MONITORING AGENCY REPORT NUMBER DOT/FRA/ORD-14/22
11. SUPPLEMENTARY NOTES COTR: Luis Maal and Ali Tajaddini	
12a. DISTRIBUTION/AVAILABILITY STATEMENT This document is available to the public through the FRA Web site at http://www.fra.dot.gov.	12b. DISTRIBUTION CODE

13. ABSTRACT (Maximum 200 words)

Detailed analysis of measured bending strains shows that the foundation deflections have the most significant effect on the magnitude of strains. All other factors, such as track type, track geometry, and fastening systems, have a less significant effect on strain levels. Fatigue analysis of the current and proposed candidate materials indicate that most joint bars may have a significantly longer fatigue life. The joint bar fatigue failures seen in service are likely from surface material discontinuities created as a result of manufacturing processes and mechanical notches induced during handling. Another factor that potentially affects the fatigue life is deteriorated foundations under rail joints. Significant residual stresses exist in as-manufactured joint bars. These stresses may affect the joint bar failures in negative or positive ways depending on the nature of service-induced stresses at a particular location. Instead of increasing the size of joint bars, managing residual stress appears to be an economical option to increase the strength of joint bars.

14. SUBJECT TERMS Strain levels, joint bar fatigue analysis, residual stress, joint bar strength	15. NUMBER OF PAGES 38
	16. PRICE CODE

17. SECURITY CLASSIFICATION OF REPORT	18. SECURITY CLASSIFICATION OF THIS PAGE	19. SECURITY CLASSIFICATION OF ABSTRACT	20. LIMITATION OF ABSTRACT
Unclassified	Unclassified	Unclassified	

NSN 7540-01-280-5500

Standard Form 298 (Rev. 2-89)
Prescribed by ANSI Std. 239-18
298-102

METRIC/ENGLISH CONVERSION FACTORS

ENGLISH TO METRIC

LENGTH (APPROXIMATE)

1 inch (in)	=	2.5 centimeters (cm)
1 foot (ft)	=	30 centimeters (cm)
1 yard (yd)	=	0.9 meter (m)
1 mile (mi)	=	1.6 kilometers (km)

AREA (APPROXIMATE)

1 square inch (sq in, in^2)	=	6.5 square centimeters (cm^2)
1 square foot (sq ft, ft^2)	=	0.09 square meter (m^2)
1 square yard (sq yd, yd^2)	=	0.8 square meter (m^2)
1 square mile (sq mi, mi^2)	=	2.6 square kilometers (km^2)
1 acre = 0.4 hectare (he)	=	4,000 square meters (m^2)

MASS - WEIGHT (APPROXIMATE)

1 ounce (oz)	=	28 grams (gm)
1 pound (lb)	=	0.45 kilogram (kg)
1 short ton = 2,000 pounds (lb)	=	0.9 tonne (t)

VOLUME (APPROXIMATE)

1 teaspoon (tsp)	=	5 milliliters (ml)
1 tablespoon (tbsp)	=	15 milliliters (ml)
1 fluid ounce (fl oz)	=	30 milliliters (ml)
1 cup (c)	=	0.24 liter (l)
1 pint (pt)	=	0.47 liter (l)
1 quart (qt)	=	0.96 liter (l)
1 gallon (gal)	=	3.8 liters (l)
1 cubic foot (cu ft, ft^3)	=	0.03 cubic meter (m^3)
1 cubic yard (cu yd, yd^3)	=	0.76 cubic meter (m^3)

TEMPERATURE (EXACT)

[(x-32)(5/9)] °F = y °C

METRIC TO ENGLISH

LENGTH (APPROXIMATE)

1 millimeter (mm)	=	0.04 inch (in)
1 centimeter (cm)	=	0.4 inch (in)
1 meter (m)	=	3.3 feet (ft)
1 meter (m)	=	1.1 yards (yd)
1 kilometer (km)	=	0.6 mile (mi)

AREA (APPROXIMATE)

1 square centimeter (cm^2)	=	0.16 square inch (sq in, in^2)
1 square meter (m^2)	=	1.2 square yards (sq yd, yd^2)
1 square kilometer (km^2)	=	0.4 square mile (sq mi, mi^2)
10,000 square meters (m^2)	=	1 hectare (ha) = 2.5 acres

MASS - WEIGHT (APPROXIMATE)

1 gram (gm)	=	0.036 ounce (oz)
1 kilogram (kg)	=	2.2 pounds (lb)
1 tonne (t)	=	1,000 kilograms (kg)
	=	1.1 short tons

VOLUME (APPROXIMATE)

1 milliliter (ml)	=	0.03 fluid ounce (fl oz)
1 liter (l)	=	2.1 pints (pt)
1 liter (l)	=	1.06 quarts (qt)
1 liter (l)	=	0.26 gallon (gal)
1 cubic meter (m^3)	=	36 cubic feet (cu ft, ft^3)
1 cubic meter (m^3)	=	1.3 cubic yards (cu yd, yd^3)

TEMPERATURE (EXACT)

[(9/5) y + 32] °C = x °F

QUICK INCH - CENTIMETER LENGTH CONVERSION

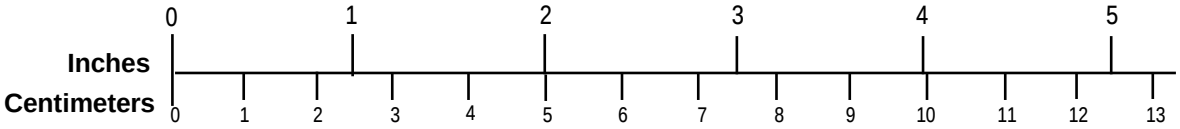

QUICK FAHRENHEIT - CELSIUS TEMPERATURE CONVERSIO

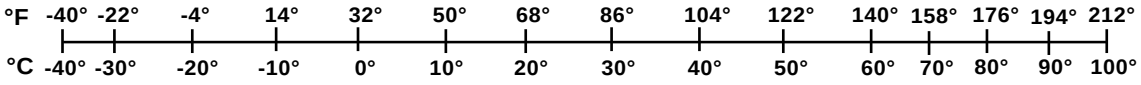

For more exact and or other conversion factors, see NIST Miscellaneous Publication 286, Units of Weights and Measures. Price $2.50 SD Catalog No. C13 10286

Updated 6/17/98

Contents

Executive Summary 1

1. Introduction 3
   1.1 Background 3
   1.2 Objectives 4

2. Statistical Analysis of Bending Stresses 5
   2.1 Test Setup 5
   2.2 Terminology—Maximum Stresses and Stress Range 7
   2.3 Maximum Bending Stresses 8
   2.4 Bending Stress Range 9
   2.5 Effects of Different Joint Bar Lengths 10
   2.6 Effects of Gage Side and Field Side Bars 12

3. Residual Stresses 16
   3.1 Measurement Procedure 16
   3.2 Data Analysis and Results 17
   3.3 Discussion 22

4. Fatigue Analysis Overview 23
   4.1 Material Properties of Joint Bars Steel 23
   4.2 Microstructure of Joint Bar Steel Materials 24
   4.3 Load Environment 25
   4.4 Development of Stress and Strain Fatigue Life Curves 25
   4.5 Fatigue Analysis 28
   4.6 Fatigue Analysis—Results 28

5. References 30

Abbreviations and Acronyms 31

Illustrations

Figure 1. A Broken Joint Bar in Service 3

Figure 2. (Top Left) Table Showing the Location of Various Test Joints, (Top Right) Sketch Shows Location of Bending Strain Gages, (Bottom) Test Joints in Track 5

Figure 3. Time History of Bending Stress on Top of the Joint Bar 6

Figure 4. Time History of Bending Stress on Bottom of the Joint Bar 6

Figure 5. Graphical Representation of Some Terms 7

Figure 6. Maximum Tensile and Compressive Stress Peaks from Wheels 8

Figure 7. Bending Stress Range of Rail Joints 9

Figure 8. Effects of Joint Bar Lengths on Bending Stress Range 10

Figure 9. Comparison of Effects of Joint Bar Lengths on Mean Bending Stress Ranges 11

Figure 10. Comparison of Effects of Joint Bar Lengths on Median Bending Stress Range and Stress Range Distribution 12

Figure 11. Bending Stress Range—Gage Side versus Field Side 13

Figure 12. Comparison of Effects of Joint Bar Insulation Type on Mean Bending Stress Range 14

Figure 13. Comparison of Effects of Joint Bar Insulation Type on Median Bending Stress Range and Stress Range Distribution 15

Figure 14. Location of Strain Gages—Clockwise from Top Left Corner—Joint Bar Cross Section, Joint Bars with the Strain Gages and Joint Bar Elevation 17

Figure 15. Residual Stresses along the Cross Section of Joint Bars 18

Figure 16. (Top) Location of Metal Flow at the Joint, (Bottom) Metal Flow on Top of the Joint Bar 19

Figure 17. (Top) Effect of Residual Stress on Stress Amplitude, (Bottom) Percentage Change in Fatigue Life with Change in Mean Stress (Note: Values May Differ According to the S-N Curve Used) 21

Figure 18. Typical Fatigue Crack in the Bottom of the Joint Bar 23

Figure 19. (Left) 1045 Steel, (Right) 4140 Steel Microstructures 25

Figure 20. Results of High Cycle Fatigue Testing 26

Figure 21. (Top) 4140 Steel, (Bottom) 1045 Steel Strain-Life Curves 27

Figure 22. Fatigue Life of Joint Bar Materials 29

Tables

Table 1. Chemical Composition of Various Joint Bar Materials 16
Table 2. Joint Bar Mechanical Properties and Chemical Composition 24

Executive Summary

The joint bar is the only track component that has not changed for many decades—the cross-section has increased to match increasing rail sizes, but the basic design has remained the same. Unlike other track components, where component-caused accidents have gradually been reduced due to design improvements, the number of joint bar related accidents has remained the same.

Under the Federal Railroad Administration (FRA) Track research program, Transportation Technology Center, Inc. (TTCI) is investigating various options to reduce joint bar failures. Under the current study, the joint bar bending stress data collected under Phase I was analyzed in more detail. The current joint bar material and a candidate material were tested in the laboratory to make S-N curves (i.e., stress against the number of cycles to failure). The S-N curves and the bending stress data were then utilized to estimate the fatigue life of both the current materials and the candidate materials. Residual stresses in most commonly used joint bars in North America were also measured by strain gaging and then saw cutting.

Statistically significant differences in bending stress range exist between joint bar types (insulated and standard), as well as joint bar lengths (36 and 48 inches). Specific tests produce different and potentially confusing results. Compound categorized plots are used to show relative variation. Means plots indicate the unexpected result of shorter joint bars experiencing a somewhat lower bending stress range than longer joint bars. Further, tests show that mean bending stress range is lower for insulated joint bars than for standard joint bars. This latter result is consistent with insulated joint bars producing bending stress ranges that have less variation and narrow distribution. However, when length is considered, short joint bars have more variation and wider distributions than do longer joint bars. This is illustrated using box and whisker plots.

It is important to consider both central tendency statistics as well as variation and distribution statistics when making comparisons of such data.

Significant residual stresses are present in most as-manufactured joint bars. Depending on the nature of the service induced residual stresses, positive or negative effect of the failure behavior of joint bars may be achieved. Compressive residual stresses in the bottom of the joint bar, where service induced stresses are tensile, can improve the yield and fatigue properties of the material. Similarly, neutralizing the residual stresses on top of the joint bar is beneficial because that location is under compression from service loads.

An obvious way to prevent joint bar failures is to increase the moment of inertia of the joint bar cross section, but that is not a practical solution because it pushes the weight of the joint bar beyond the manual handling limits. By properly managing the residual stresses, which are significant in the as-manufactured joint bars, some joint bar failures may be prevented. Increasing joint bar mechanical properties is also an option.

The fatigue life of the current standard joint bar is estimated to be more than 2,000 million gross tons (MGT). Considering tonnage on most routes, this is practically infinite fatigue life. The estimated life of insulated joint bars is even higher than that of standard joint bars. The loading data used for this analysis was collected from various types of joints installed and maintained in Class 4 track. The rail joints that operate on deteriorated foundations are likely to experience higher stresses and thus lower fatigue life. The effects of surface discontinuities in the material

and mechanical notches induced during handling were not considered in the analysis. Most fatigue failures that occur on well-maintained track may be the result of these two factors.

The yield strength of a rail joint bar has been traditionally lower than the surrounding rail. This is largely due to the common perception that increased yield strength may reduce the fracture toughness and fatigue life of joint bar materials, but experimental results do not show this to be correct for modern steels. The yield strength of a proposed candidate material is 70 percent higher and the fracture toughness is 60 percent higher than current joint bar material. The estimated fatigue life of the candidate material is similar to that of the current material.

In the next phase of this study, the effects of various track maintenance procedures for joint failures will be studied. The benefits of using larger bolts and having smaller gaps will be evaluated. Also, various options to reduce existing in-track joint bar failures will be studied. The contact stresses at the joint bar top and rail interface are difficult to measure. Finite element methods will be used to estimate these stresses.

1. Introduction

Joint bar design may be the only track component design that has not changed for many decades. Joint bar cross sections have usually increased to match the increasing rail sizes, but the basic joint bar design has remained the same. Other track component-caused accidents have gradually been reduced because of design improvements, but the number of joint-bar-related accidents has remained the same.

Generally, joint bar failures, both in bolted and insulated joint bars, are caused by fatigue. Fatigue causes crack initiation, and with additional loads, the crack can grow and cause failure. Many derailments and accidents have been caused by joint bar failure.

The following activities were performed to achieve the objectives of this study:

- Statistical analysis of bending strain data collected during first phase of this task order;
- Residual stress measurements in joint bars collected from most of the manufacturers;
- Fatigue analysis of joint bars using collected load environment data and material test data; and
- Failure analysis of cracked and broken joint bars found during track inspections.

Figure 1. A Broken Joint Bar in Service

1.1 Background

Past research on track components has focused mostly on improving rail integrity, resulting in improved rail performance under the increased axle loads of today's rolling stock. Joint bars, which are used to join the rails, have not been studied in equal detail. The last documented detailed research was conducted in the 1920s by the American Railway Engineering Association (now the American Railway Engineering and Maintenance-of-Way Association (AREMA))

committee on track stresses. Unlike rail that is removed mostly due to wear, joint bars are removed because of fatigue cracking or breaking. A cracked joint bar may remain in track for some time before it is detected and removed. During that time, the joint bar poses a higher safety risk. At the very least, a cracked or broken joint bar can create very high impact loads, which may cause damage to the track foundation and to rolling stock.

Two types of rail joints, bolted and insulated joints, perform differently and have different operational objectives; however, they share many similar design features. For example, they are butt joints of the rail and both use bolts and bars to connect the two rails. A butt joint creates a discontinuity or gap in the running surface of the track on each rail. The discontinuity in the running surface of the rail creates conditions that can accelerate track degradation around the joint. At a minimum, the gap at the rail ends within the rail joint is a source of impact loading from passing wheels. Left unchecked, these impact loads increase rail end batter, thereby deteriorating the foundations and further increasing the impact forces generated by passing wheels. Like other special trackwork components, rail joints have a much lower average service life than the parent rail. At the same location, a rail joint may be replaced many times during the service life of the surrounding rail.

1.2 Objectives

Work performed under this task order aimed to recommend guidelines for new joint bar design using the following:

- The statistical analysis of load environment data;
- Fatigue analysis of current and proposed joint bar materials;
- Residual stress measurements of joint bars; and
- Failure analysis of failed joint bars.

2. Statistical Analysis of Bending Stresses

Statistical difference tests were run on the data to compare stresses between different combinations of pairs of joint bar groups (e.g., 36 and 48 inches, wood tie and concrete tie, insulated and standard, etc.). A mix of parametric (Gaussian or normally distributed data) and nonparametric (not normally distributed data) comparison tests was used because the various datasets did not consistently display either normal or nonnormal distribution characteristics. The parametric tests were accepted as reasonable because histograms of most subsets appeared to be normal in shape and symmetry. Multiple tests were run, including ANOVA and the Kruskal-Wallis ANOVA & Median test, from which mean error plots will be shown.

2.1 Test Setup

Bending strains were collected on 16 rail joints under several trains at FRA's Facility for Accelerated Service Testing (FAST) near Pueblo, CO. Each joint had four bending circuits—two at the top of the joint bar and two at the bottom. Half of the joints were located on a curve and half were located on tangent track. All of the joints were installed as suspended (i.e., the end post was at the center of the ballast crib). Figure 2 shows a typical test joint layout in track.

Strain gages were used to measure bending strains at 25 to 30 MGT intervals. The FAST train operates 315,000-pound cars at speeds between 40 and 45 miles per hour (mph).

Wood Tie Tangent	Wood Tie Curve	Concrete Tie Tangent	Concrete Tie Track
48" IJ	48" IJ	48" IJ	48" IJ
36" IJ	36" IJ	36" IJ	36" IJ
48" Std.	48" Std.	48" Std.	48" Std.
36" Std.	36" Std.	36" Std.	36" Std.

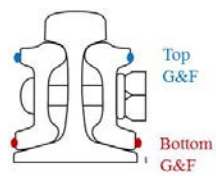

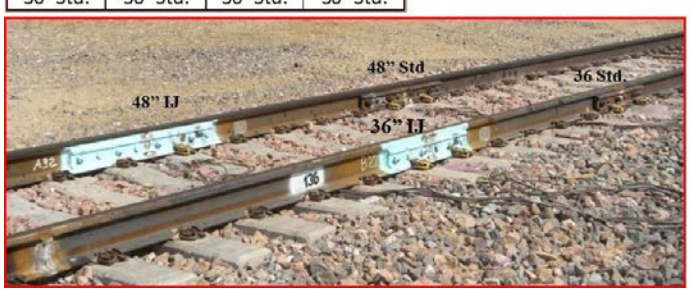

Figure 2. (Top Left) Table Showing the Location of Various Test Joints, (Top Right) Sketch Shows Location of Bending Strain Gages, (Bottom) Test Joints in Track

Figures 3 and 4 show typical bending strain history for joint bar tops and bottoms. As the plot shows, the joint bar bottom experiences mostly tension, but also some compressive stresses. The joint bar top experiences mostly compressive, but also some tensile stresses because moving wheels cause positive and negative bending in the rail joints.

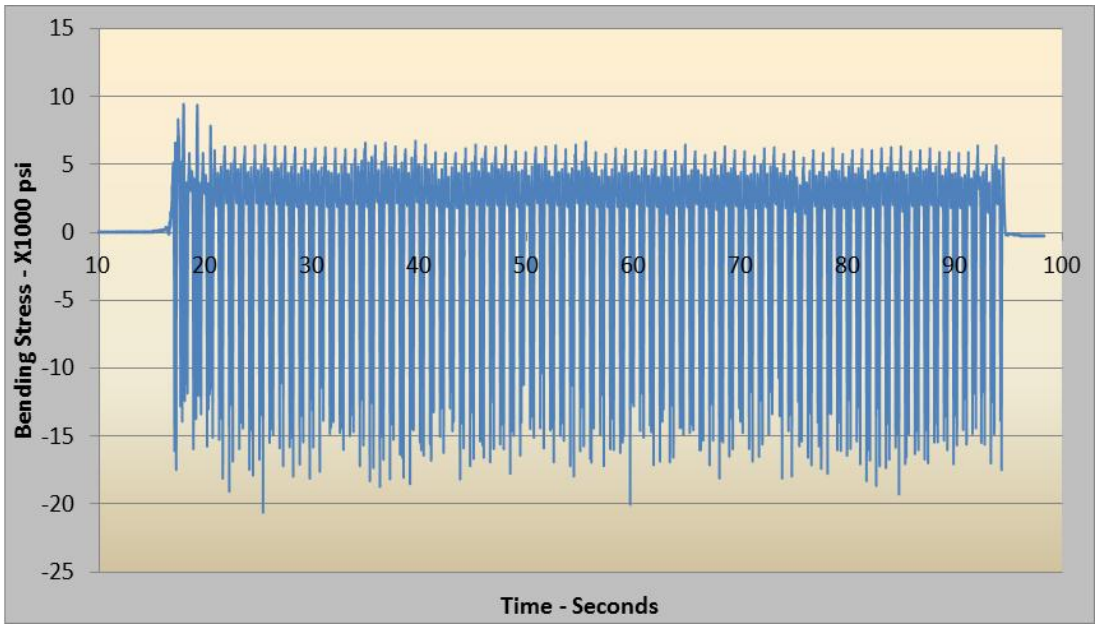

Figure 3. Time History of Bending Stress on Top of the Joint Bar

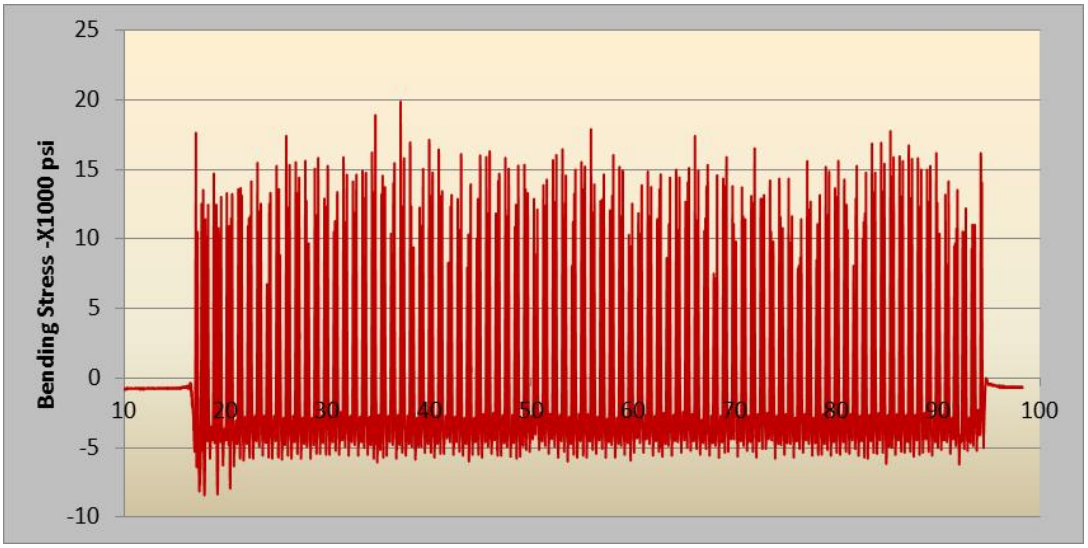

Figure 4. Time History of Bending Stress on Bottom of the Joint Bar

2.2 Terminology—Maximum Stresses and Stress Range

When a wheel is on the top of the rail joint, it causes compressive bending stresses on the top and tensile bending stresses on the bottom. As the wheel moves toward or away from the rail joint, it reverses the stresses (i.e., compressive stress is induced in the tensile zone and tensile stress is induced in the compression zone). This condition is known as negative bending. Negative bending affects the stress range, which is required for fatigue analysis. Each wheel creates one spike of compressive stress on top and one spike of tensile stress. This is called maximum or peak stress. Figure 5 shows, graphically, the meaning of various terms. Stress range is the difference of maximum and minimum stresses and is always an absolute value. Maximum stress can be either positive or negative, depending on if the stress is compressive or tensile.

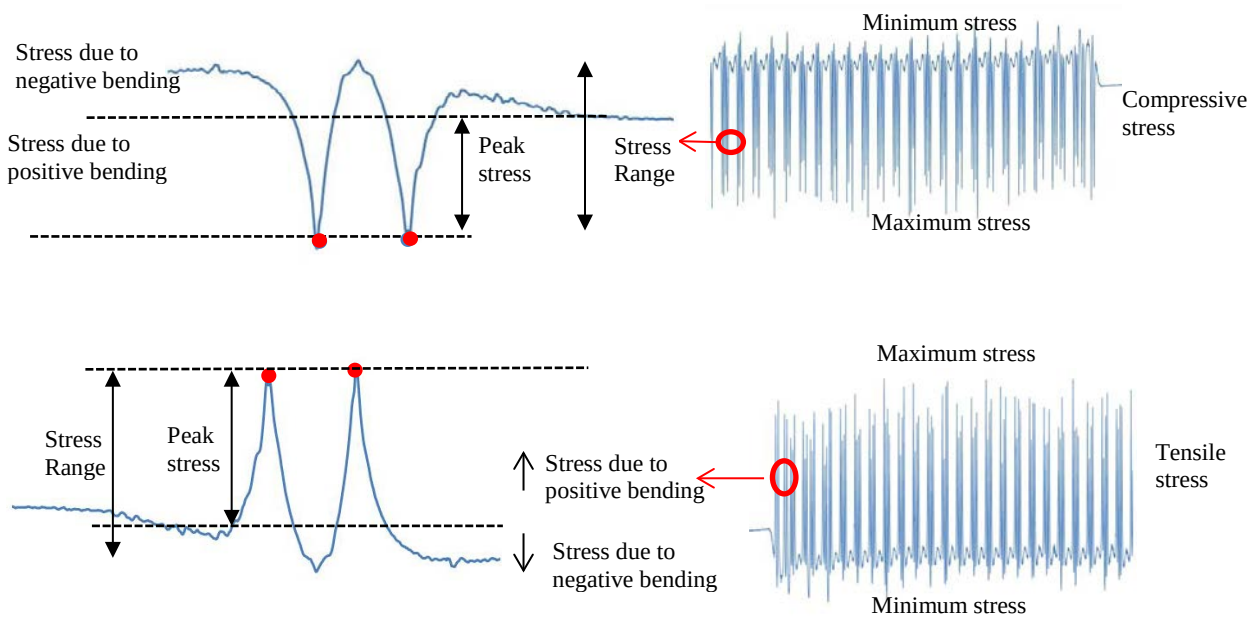

Figure 5. Graphical Representation of Some Terms

2.3 Maximum Bending Stresses

Four different types of rail joints at four different locations accumulated 100 MGT traffic under the FAST train. Bending strains were collected under three train passes at four different tonnage intervals (8, 36, 73, and 102 MGT). For each train's time-strain history, maximum compressive and tensile strain (peak) generated by each wheel were calculated. Figure 6 shows the combined plot of the peak data collected at all 16 joint bar locations. Each column is the sum of many data points representing a peak tensile or compressive force stress measurement collected at each strain gage (top or bottom of joint). Strain gages on the top show predominantly compressive stresses and the ones on the bottom show tensile stresses.

The joints were installed on track that was maintained per Class 4 standards.

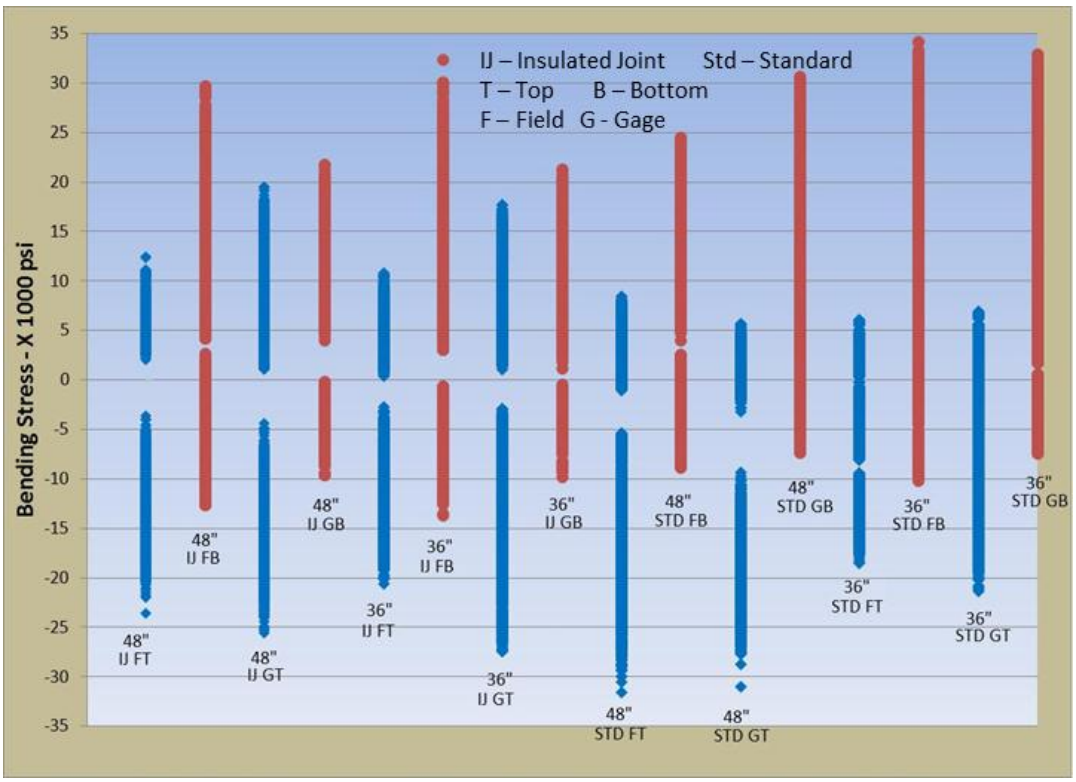

Figure 6. Maximum Tensile and Compressive Stress Peaks from Wheels

2.4 Bending Stress Range

Stress range data for the four strain gages on each joint were combined to generate one histogram for each joint. Figure 7 shows the bending stress range of all 16 joints. Because the stress range is the absolute difference of maximum and minimum stresses, compressive and tensile bending stresses both have positive sign convention. Stress range does not show which type of joints typically had higher or lower stresses. This may suggest that the effect of local foundation conditions is greater than the effects of rail joint type and length.

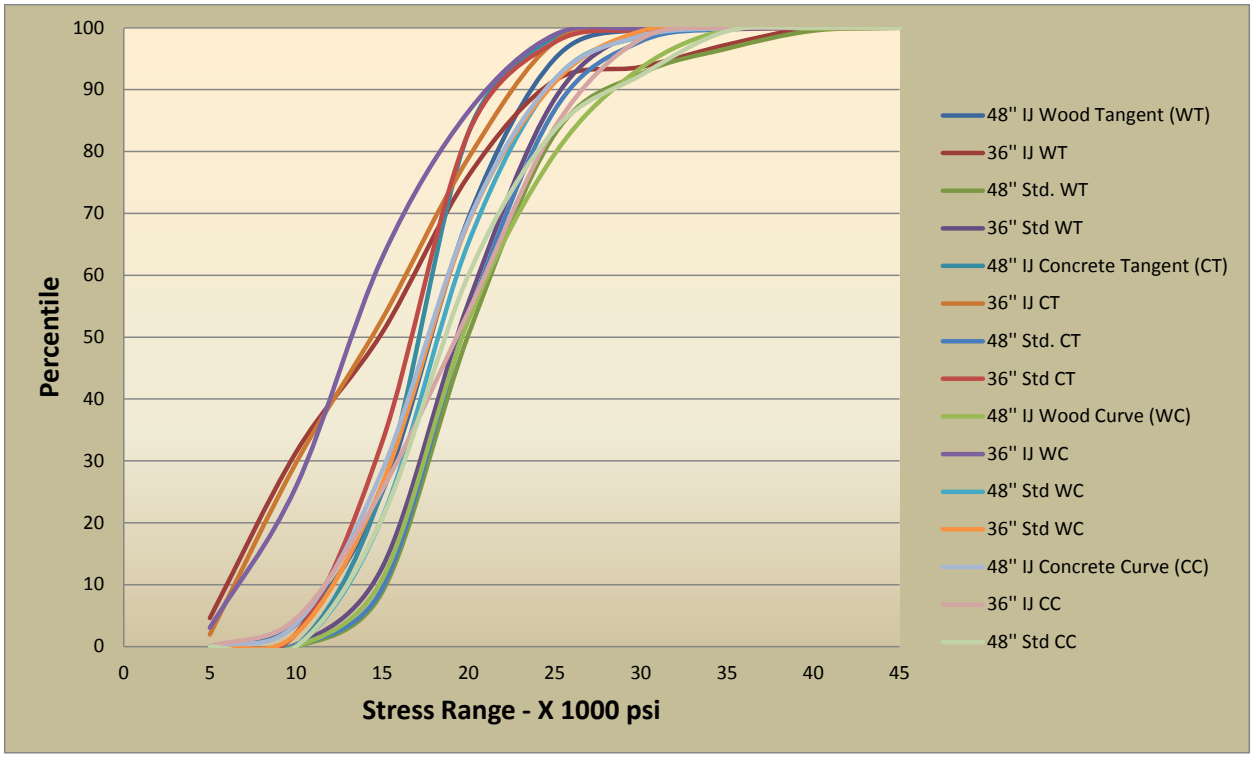

Figure 7. Bending Stress Range of Rail Joints

2.5 Effects of Different Joint Bar Length

Figure 8 shows the effects of 36- and 48-inch-long standard and insulated joints on the bending stresses at different track geometry locations. At the bottom left, the graph shows that the stress ranges of 36- and 48-inch-long insulated joint bars were similar. The bottom right graph shows that the stress range of 48-inch-long joint bars was always higher than that of 36-inch-long joint bars. The top two graphs show that regardless of length, the stress range of standard joint bars was mostly higher than that of insulated joint bars.

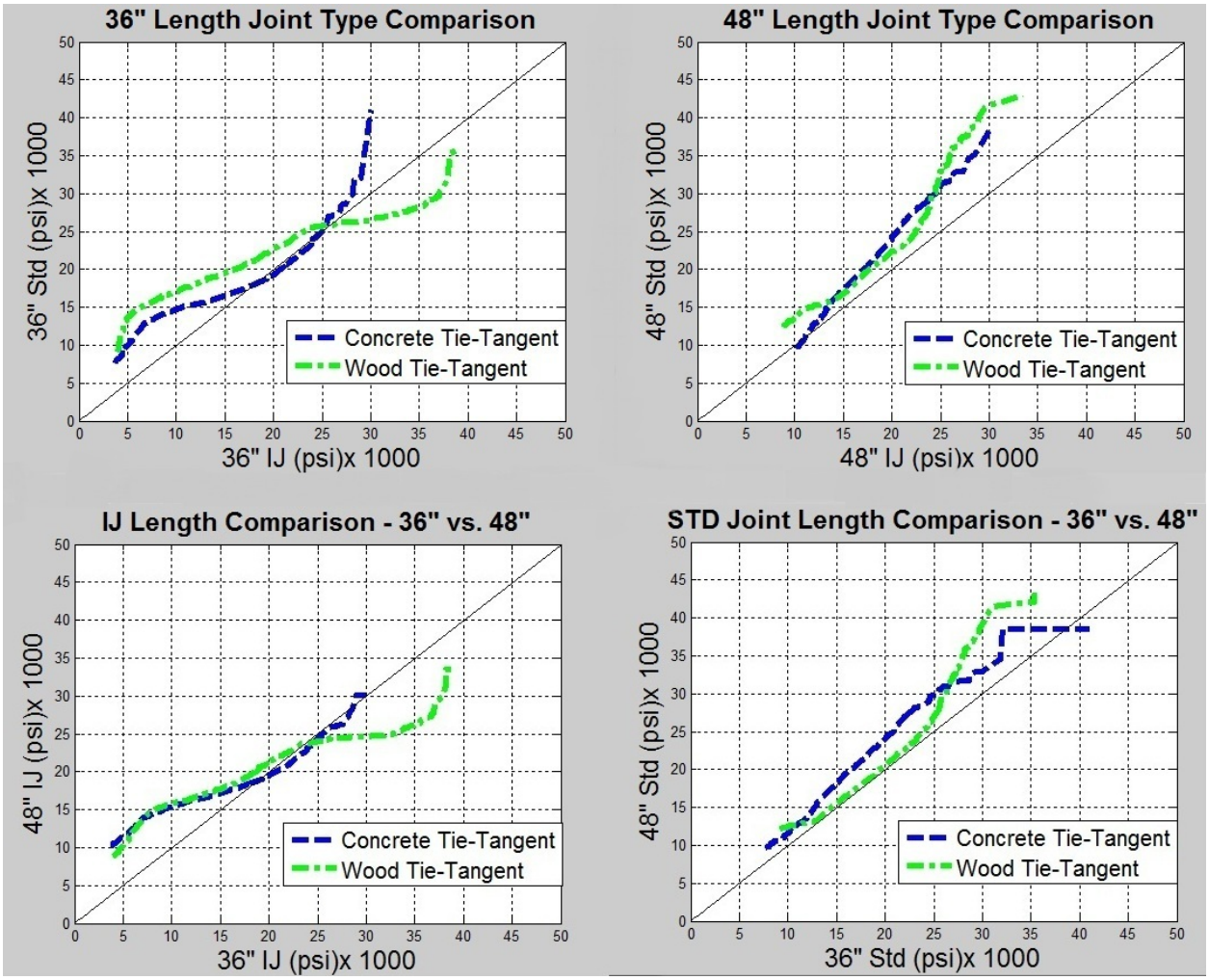

Figure 8. Effects of Joint Bar Lengths on Bending Stress Range

Figure 9 is a categorized stress range mean graph showing comparisons between joint bar length (represented by the number of bolt holes: 6 = 36 inches; 8 = 48 inches), insulation type (insulated or standard), and track location (curve or tangent). It shows that the shorter joint bars experience lower average stress ranges than the longer bars do. The upper right graph does not show the same distinctive difference as the other categories because one standard 6-hole joint bar sample from concrete tie in curved track showed inconsistent differences, leading to inconclusive results. Nevertheless, this inconsistency does not invalidate the results of the other samples, where the differences are statistically significant at the 95 percent confidence level (*p-value* ≤ 0.05).

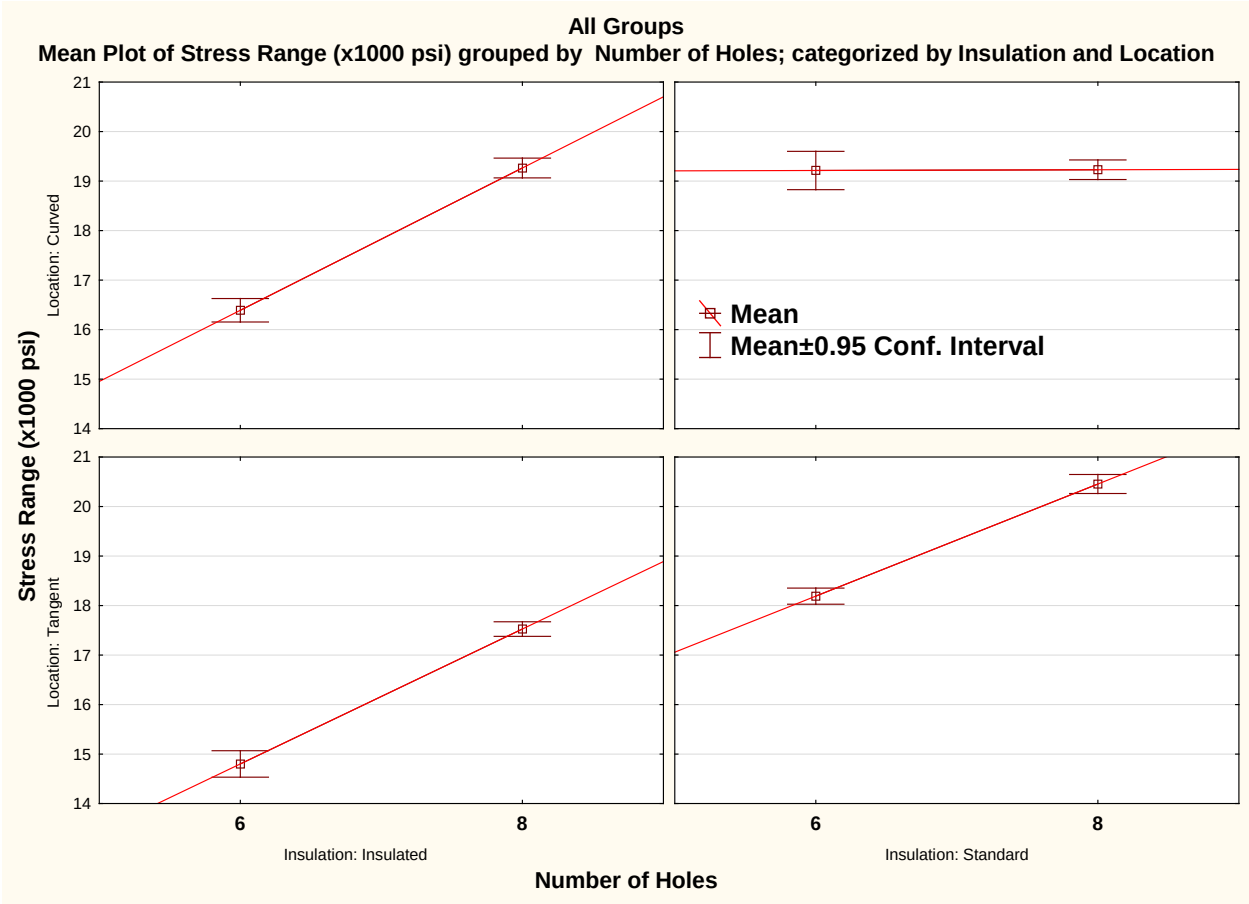

Figure 9. Comparison of Effects of Joint Bar Lengths on Mean Bending Stress Ranges

The mean stress range plots in Figure 9 indicate the *central tendency* of the respective bending stress ranges by different factor combinations. However, these do not provide indications of relative variations or the overall range of stresses themselves. The box and whisker plots of Figure 10 provide more complete characteristics of both location (median) and variation (25 to 75 percent box or interquartile range) of bending stress ranges along with the broader distribution of the stress range (5 to 95 percent whiskers or 90 percent of the bending stress range). Only tangent data is compared.

In Figure 10, the top row of subplots shows concrete tie track data, the bottom row shows wood tie track data, the left column shows insulated joint data, and the right column shows standard joint data. For the insulated joint bars (left column plots), the longer joint bars show lower variation and narrower distribution on both concrete and wood tie track, relative to the Y-axis. The interquartile ranges (boxes) are shorter and 90 percent of the distribution (whiskers) is smaller for 8-hole versus 6-hole joint bars. For standard joint bars (the right subplot column), the difference is less distinctive and is inconsistent. The interquartile ranges look similar, whereas 90 percent of the distribution appears larger for longer, 8-hole joint bars.

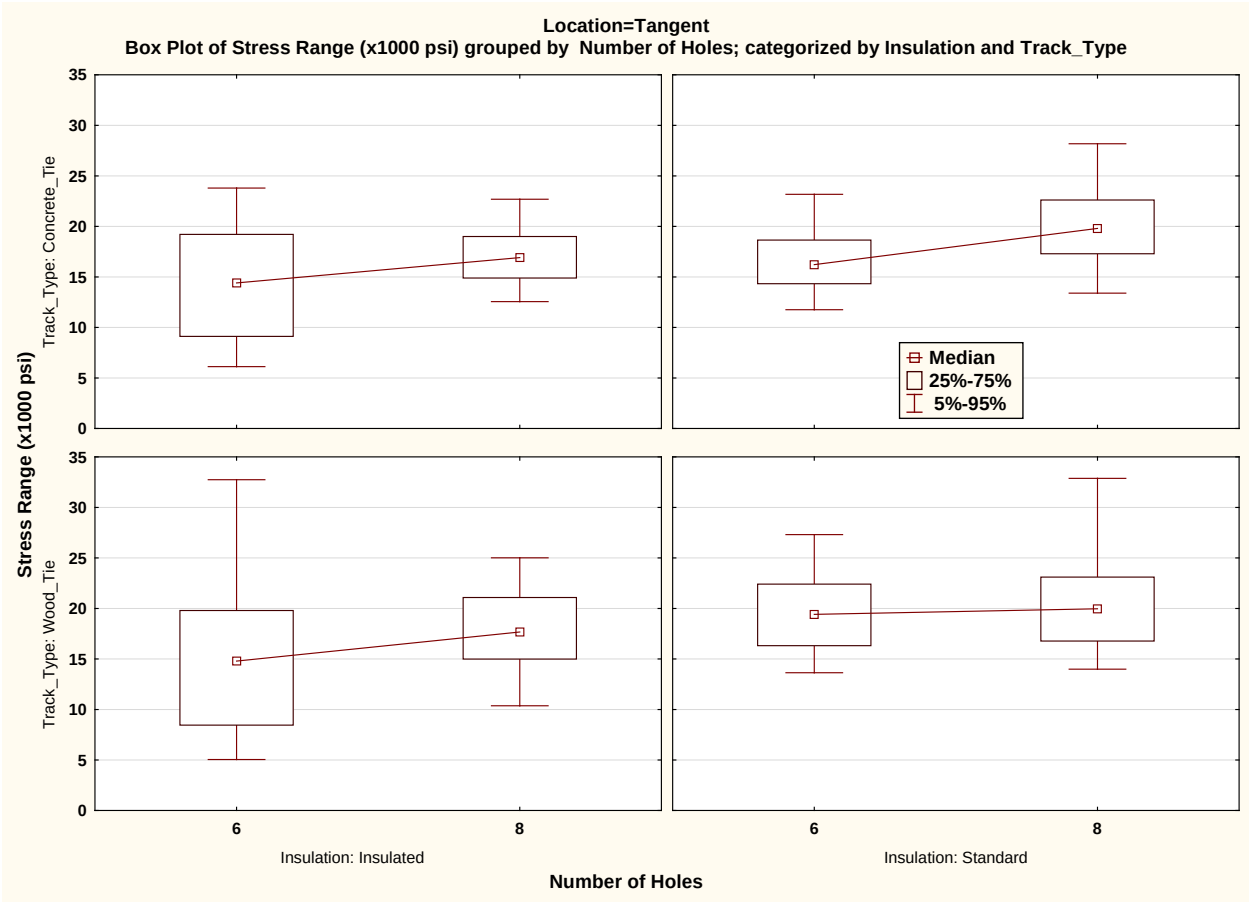

Figure 10. Comparison of Effects of Joint Bar Lengths on Median Bending Stress Range and Stress Range Distribution

2.6 Effects of Gage Side and Field Side Bars

Theoretically, both joint bars of a rail joint should have similar stresses under load. However, in reality, that is not the case, as Figure 11 shows. Bending stresses in one joint bar can be up to 40 percent higher or lower than that of the other joint bar. This difference in stress levels between the field side and gage side of the joint bars is likely due to vehicle dynamics, component tolerances, or differences in bolt torque, which change over time.

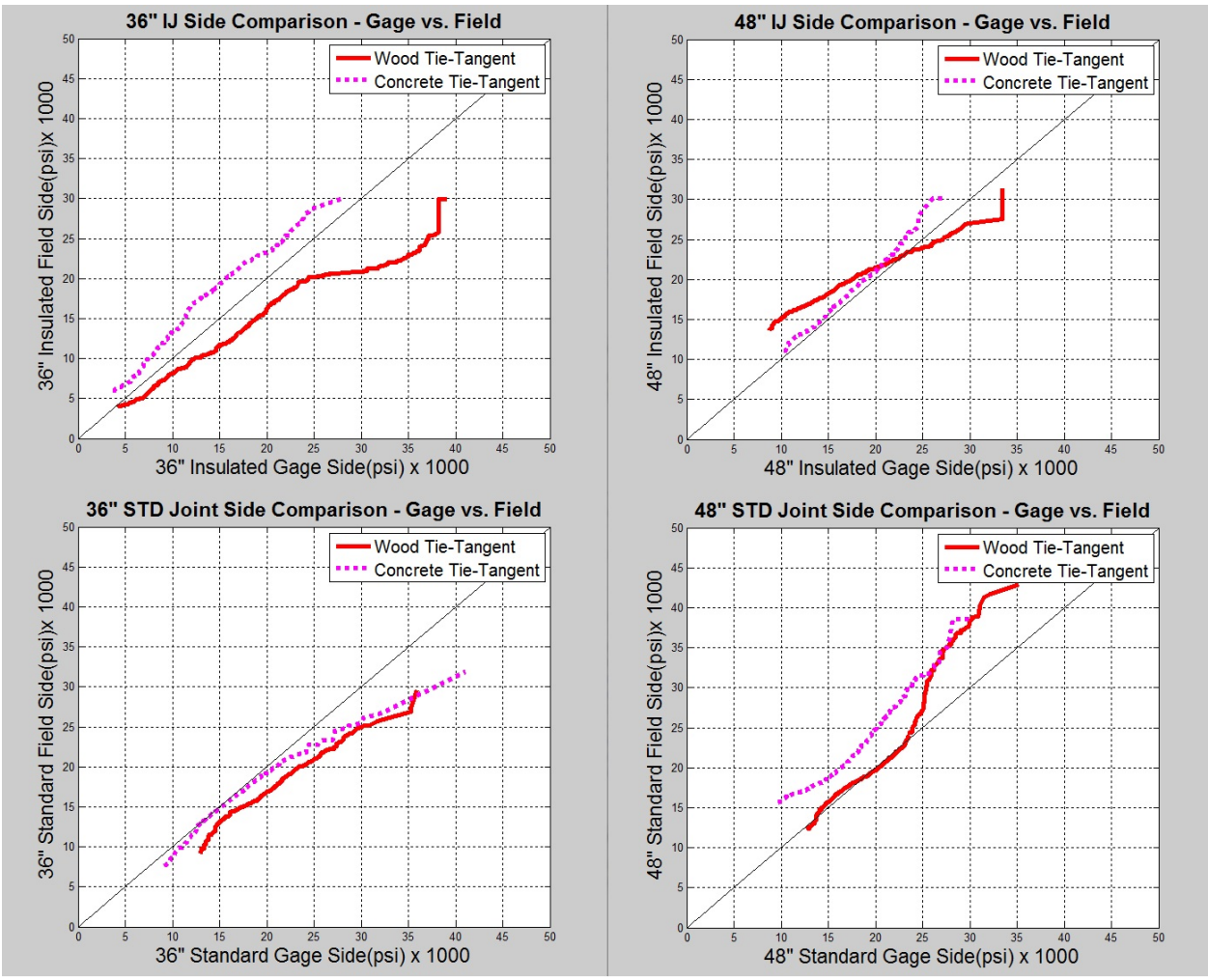

Figure 11. Bending Stress Range—Gage Side versus Field Side

2.7 Insulated and Standard Joints

Figure 12 is a categorized stress range mean graph showing comparisons between insulation type (insulated or standard), joint bar length (represented by the number of bolt holes: 6 = 36 inches; 8 = 48 inches), and track location (curve or tangent). The plots show that insulated joint bars experience lower stress ranges than standard joint bars do. The upper right subplot does not show the same distinctive difference as do the other subplots because one 8-hole insulated joint bar sample from wood tie in curved track showed inconsistent differences, leading to inconclusive results. For the rest of the plots, the differences are statistically significantly at the 95 percent confidence level (*p-value* ≤ 0.05).

Figure 12. Comparison of Effects of Joint Bar Insulation Type on Mean Bending Stress Range

The stress range mean plots in Figure 12 and the box and whisker plots of Figure 13 indicate the same relative relationships of the respective bending stress ranges by different factor combinations. In general, the insulated joint bars have lower mean or median bending stress ranges, as indicated by the slope of the connecting lines between means or medians. Only tangent data are compared.

The Figure 13 rows of subplots are data collected from concrete tie track and from wood tie track, respectively. The left column is from 6-hole joints, and the right column is from 8-hole joints.

From the left column, or 6-hole joint bars, the insulated joint bars show greater variation and wider distribution on both concrete and wood tie track. The opposite is the case for longer or 8-hole joint bars (the right subplot column). The insulated joint bars show lower variation and narrower distribution than the standard joint bars.

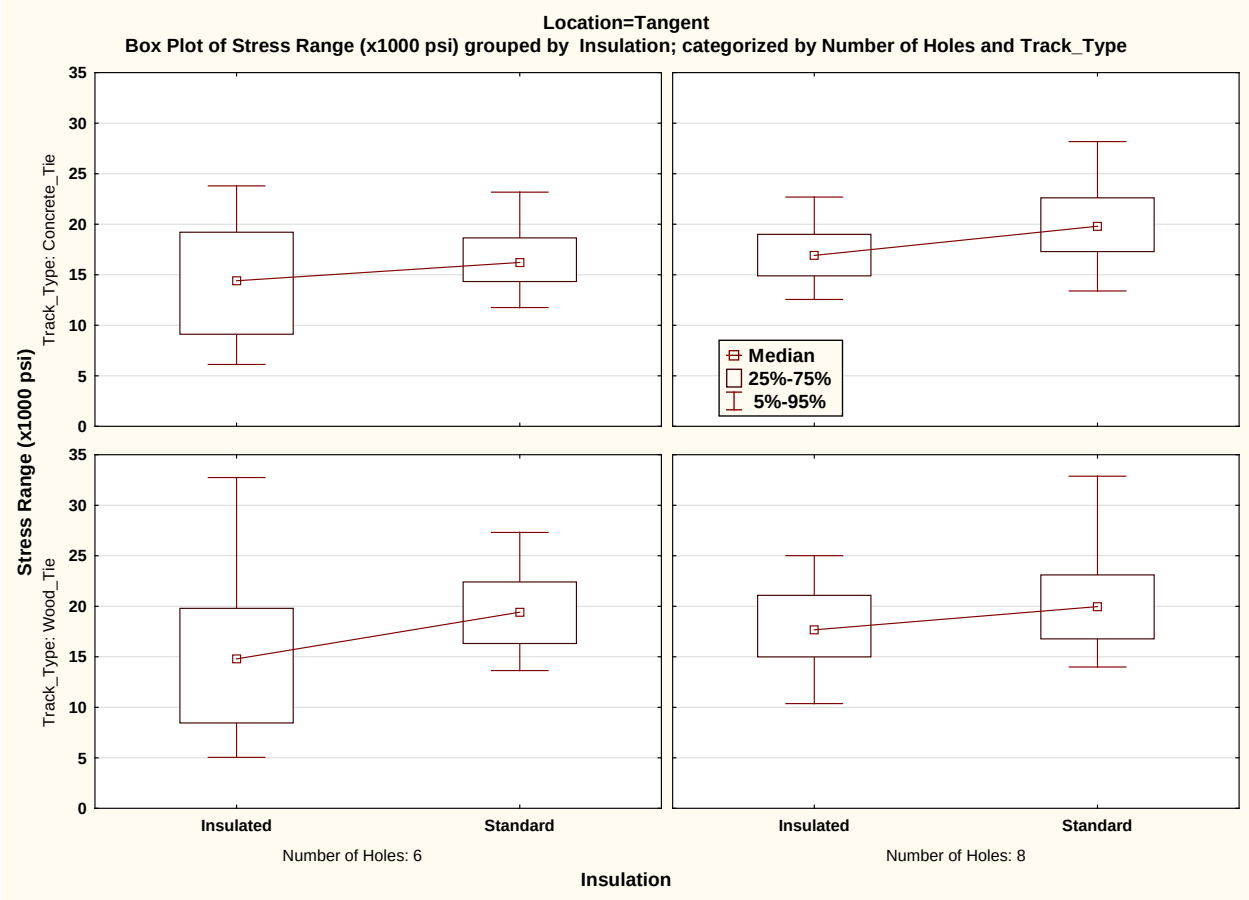

Figure 13. Comparison of Effects of Joint Bar Insulation Type on Median Bending Stress Range and Stress Range Distribution

2.8 Discussion and Conclusions

This study shows that there are statistically significant differences in stress by length of joint bar or type (insulated or standard). However, these differences must be appropriately qualified. Certain statistical tests compare the central tendency (as illustrated by categorized mean plots, Figures 9 and 12). Other tests distinguish statistically significant differences between data samples by level and type of dispersion or variation (as illustrated by categorized nonparametric box and whisker plots, Figures 10 and 13).

For the samples analyzed, central tendency comparisons show mean bending stress range values to be slightly higher for longer (48 inches) joint bars than for shorter ones (36 inches), irrespective of joint bar type. Mean bending stress ranges are greater for standard joint bars than for insulated joint bars, irrespective of length.

However, when comparing the sample data for nonparametric (non-Gaussian or distribution-type independent) dispersion characteristics, different relationships arise. Longer joint bars from the sample exhibit much less variation and a narrower range of bending stresses than do shorter joint bars. Insulated joint bars show the same reduced variation and limited range as standard joint bar bending stresses. These relationships hold for both concrete and wood tie track.

3. Residual Stresses

Residual stresses in most manufactured parts have the potential to improve or diminish the fatigue life of components subjected to millions of load cycles. Residual stresses can be detrimental if these stresses are similar to stresses induced by service loads. For example, if a location in a certain part is subjected to tensile stresses from service loads, then tensile residual stresses will reduce the useable material yield strength. However, if the same location has tensile stresses from service loads, then compressive residual stresses will be useful because they will increase the yield capacity of the component. The next section shows the procedure to measure residual stresses and how they affect the fatigue and yield properties of the joint bar material.

3.1 Measurement Procedure

AREMA recommends carbon steel and micro alloyed steel for joint bars. Carbon steel is quenched to improve the microstructure. Holes are hot punched in carbon steel joint bars during the quenching process. The holes can be cold drilled or hot punched, depending on whether or not the microalloyed steel joint bars are quenched. Quenched joint bars may be cold straightened to meet AREMA alignment tolerances. Table 1 shows the composition of joint bar steel acquired for measurement of residual stresses. Table 1 also shows if the material was quenched or not. All joint bars were made for 132-136-141 RE rail. The joint bar basic geometrical design conforms to AREMA recommendations.

Table 1. Chemical Composition of Various Joint Bar Materials

	Supplier 1	**Supplier 2**	**Supplier 3**	**Supplier 4**
Carbon	0.44	0.5	0.32	0.24
Manganese	0.73	0.61	1.38	1.45
Phosphorus	0.016	0.012	0.012	0.016
Sulfur	0.024	0.024	0.01	0.007
Silicon	-	-	0.32	0.27
Copper	-	-	0.03	0.33
Nickel	-	-	-	0.1
Chromium	-	-	0.2	0.1
Molybdenum	-	-	-	0.021
Vanadium	-	-	-	0.076
Aluminum	-	-	-	0.009
Quenched	Yes	Yes	Yes	No

Six joint bars from four different sources were acquired for this study. The procedure used to measure residual stresses is a destructive process called sectioning. In this process, strain gages are installed and the component is saw cut. The difference in strains before and after cutting is the magnitude of residual stresses.

In the study, five strain gages were installed across the cross section of 24 joint bars. The strain gages used were single element and measure strain changes in one direction. All strain gages

were located in the longitudinal center of the joint bars. This is the location where highest stresses are expected. Figure 14 shows this arrangement.

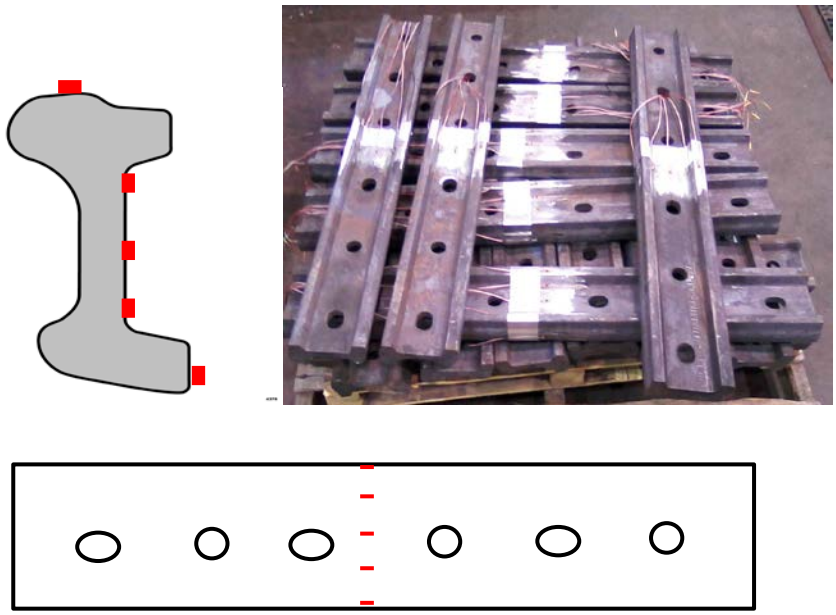

Figure 14. Location of Strain Gages – Clockwise From Top Left Corner – Joint Bar Cross Section, Joint Bars with the Strain Gages and Joint Bar Elevation

All joint bars were saw cut one-eighth of an inch away from strain gages. Strains were measured before and after the saw cut.

3.2 Data Analysis and Results

Each data point in Figure 15 shows the average stress measured at the different locations for all six joint bars from each supplier. All carbon-quenched joint bars had significant residual stresses on the tops and bottoms. Microalloyed steel joint bars (supplier 4) showed the lowest residual stresses.

Compressive residual stresses develop in joint bars because of the different rates of cooling for the various parts. The top and bottom edges have higher surface-to-weight ratio, thus the cooling rate is higher and compressive residual stresses develop on the top and bottom of the bar.

Another reason for residual stress development is the handling during quenching. Multiple joint bars are thrown in the quenching tank, mostly one on top of the other. This causes the joint bar to bend in the direction of least resistance during cooling.

AREMA recommends a “zero” dip and maximum of 0.030-inch crown on an assembled joint. Also, horizontal deviation of the center of the joint from a straight line is recommended to be less than 0.040-inch. The same tolerances are normally applied to individual joint bars. To keep the distortions within AREMA recommended tolerances, manufacturers cold straighten the joint bars after heat treatment. The cold straightening process is also believed to develop residual stresses.

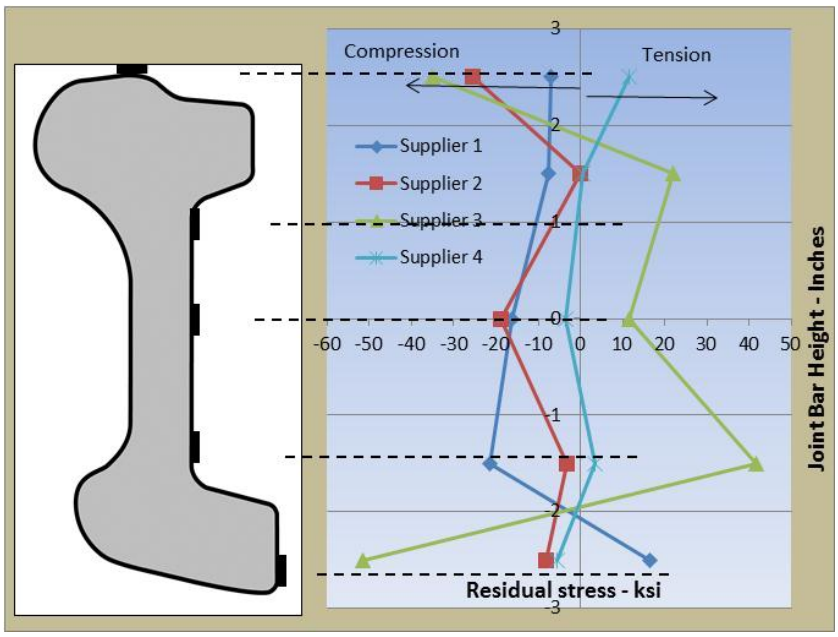

Figure 15. Residual Stresses along the Cross Section of Joint Bars

3.2.1 Effects of Residual Stresses on Yield Strength of Steel

Tops and bottoms of joint bars are subjected to the highest stresses and thus are most affected by residual stresses. Service loads induce tensile bending stresses on the bottoms of the joint bars. Thus, a compressive residual stress on the bottom will increase the ability of the material to endure higher stresses at the bottom of the joint bar, which in turn is a beneficial and desired feature. However, tensile residual stress will reduce the yield capacity of the steel and is therefore not beneficial. For example, if bending tensile stress is 20,000 pounds per square inch (psi) and compressive residual stress is 15,000 psi, the net tensile stress in the bottom of the joint bar will only be 5,000 psi. Similarly, if the bottom has a tensile residual stress of 15,000 psi and is also subjected to a bending tensile stress of 20,000 psi, the total stress will be 35,000 psi.

The top of joint bars is subjected to compressive bending stresses. If this bending stress is 20,000 psi and there is compressive residual stress of 15,000 psi, the result will be a net 35,000 psi compressive stress. On the other hand, if the top has 20,000 psi and there is tensile residual stress of 15,000 psi, then the result will be a net 5,000 psi compressive stress.

The tops of the joint bars are under very high contact stresses because of contact with the rail ends. These contact stresses are compressive in nature. As Figure 15 shows, residual stresses on top are compressive as well. The total effect of compressive residual stresses and contact stresses causes metal flow on the top of the joint bar, as Figure 16 shows. This metal flow is a likely cause of crack initiation. This metal flow may be reduced by decreasing compressive residual stresses on the top of the joint bar.

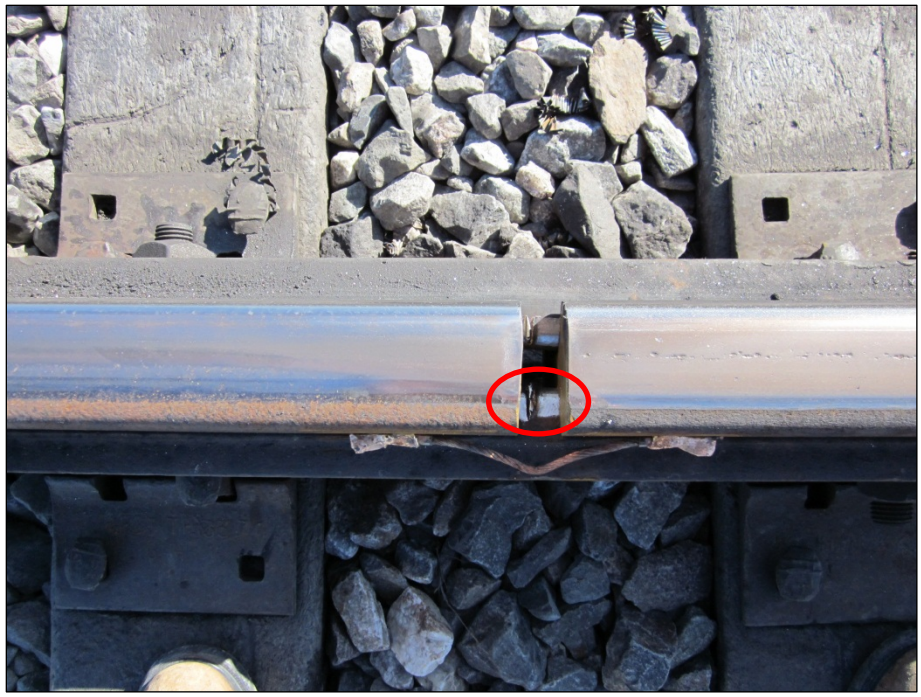

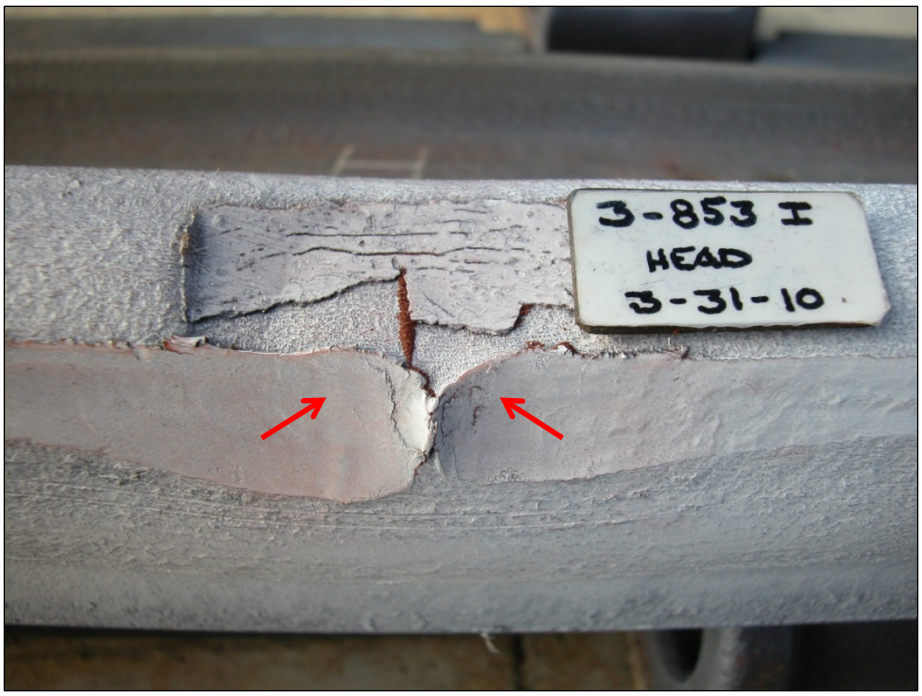

Figure 16. (Top) Location of Metal Flow at the Joint, (Bottom) Metal Flow on Top of the Joint Bar

3.2.2 Effects of Residual Stresses on Fatigue Life

Two types of stresses that are used for fatigue life estimation are stress amplitude (or stress range) and mean stress. Stress range was defined in Figure 5. Mean stress is the average of stress and can be tensile or compressive. A tensile mean stress reduces the fatigue life and a compressive mean stress increases the fatigue life. Residual stresses affect the mean stress used for fatigue calculations. Therefore, a compressive residual stress will increase the fatigue life and vice versa.

Equation 1 is the general form of a modified Goodman equation, which can be used analytically to calculate fatigue life in terms of cycles. In the equation, $\sigma_m$is mean stress, σ_e is stress amplitude when mean stress is zero, and σ_a is stress amplitude when mean stress is not zero. UTS is the ultimate tensile strength of material.

$$\sigma_a = \sigma_e \left(1 - \frac{\sigma_m}{UTS}\right) \qquad (1)$$

Figure 17 (top) shows the variation in stress amplitude when mean stresses are considered in the above equation. Using a typical S-N curve equation ($N=aS^b$), Figure 17 (bottom) shows the service life in cycles with increase and decrease in stress amplitude.

As an example, a tensile residual stress of 20,000 psi is likely to increase the stress amplitude from 20,000 psi to approximately 23,000 psi, as shown in Figure 17 (top). This increase in stress amplitude is likely to reduce fatigue life by 50 percent. Similarly, a compressive residual stress of -20,000 psi will reduce the stress amplitude to 17,000 psi, with a 100 percent corresponding increase in fatigue life.

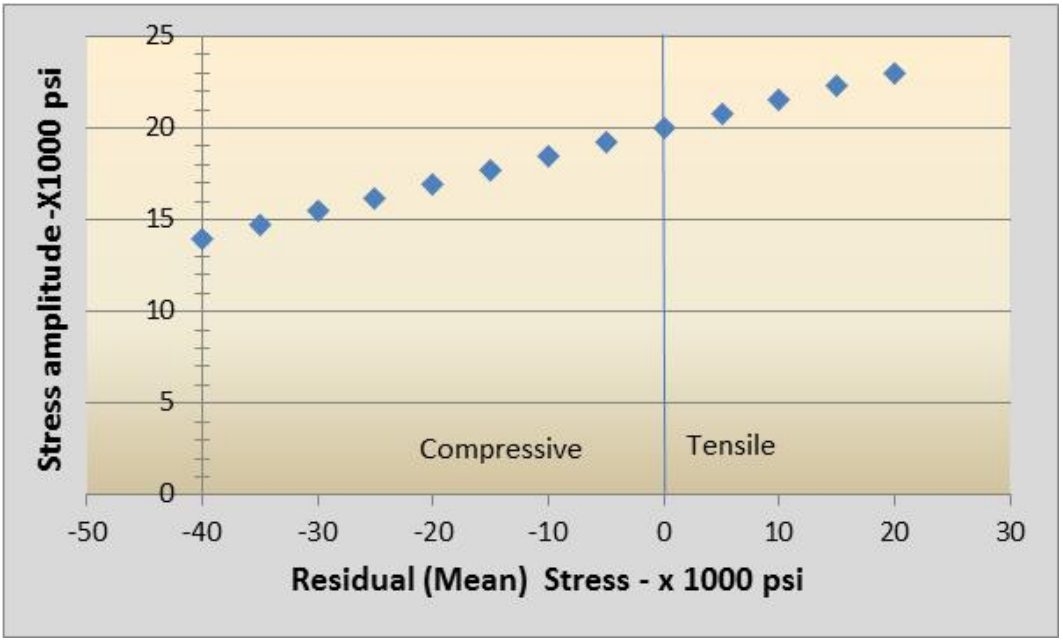

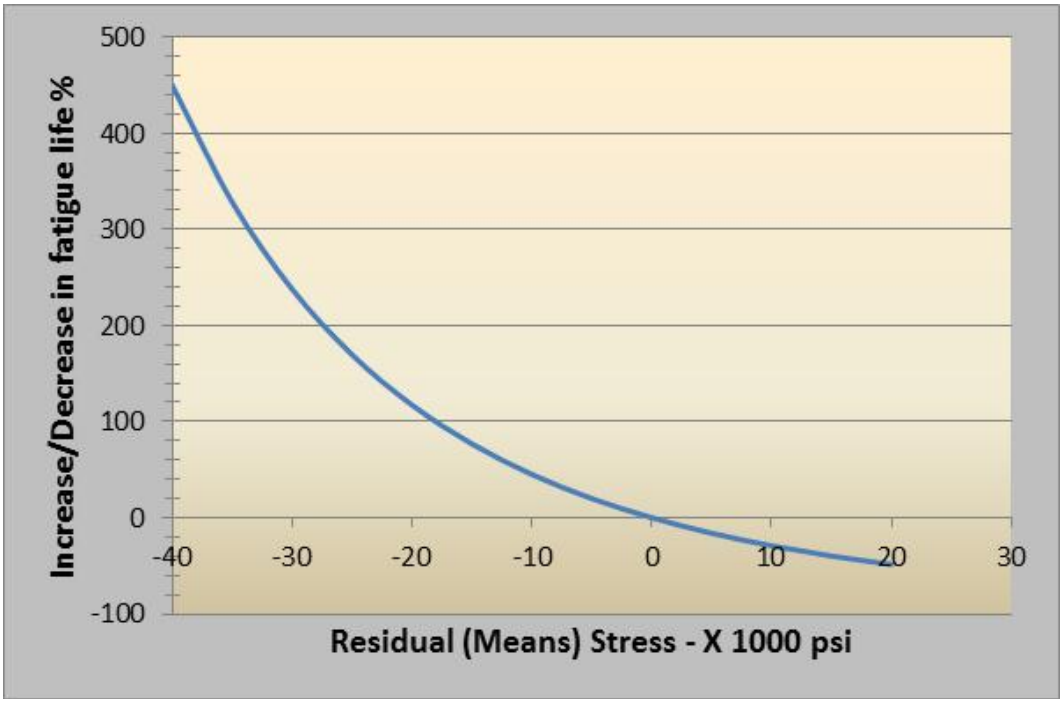

Figure 17. (Top) Effect of Residual Stress on Stress Amplitude, (Bottom) Percentage Change in Fatigue Life with Change in Mean Stress (Note: Values May Differ According to the S-N Curve Used)

3.3 Discussion and Conclusions

As explained in section 3.2.1, the top of the joint bar is subjected to compressive stresses, so tensile residual stress is likely to increase the load-carrying capability of material on top of the joint bar. It was also mentioned in section 3.2.2 that a tensile residual stress is expected to reduce fatigue life on the same location of the joint bar. The logical choice is to neutralize residual stresses at this location.

At the bottom of the joint bar, which is subjected to tensile bending stresses, a compressive residual stress is likely to increase the load-carrying capability as well as the fatigue life of joint bars. Most quenched joint bars normally have significant residual compressive stresses that are beneficial for the joint bars. However, some joint bars carry tensile residual stresses in the bottom of the joint bars, which has a negative effect on the service life of joint bars.

Ideally, one cost-effective way of increasing joint bar service life is to induce compressive residual stresses in the bottom and neutralize stresses on top. Stresses can be neutralized by partially heating the component to 1150 ºF and cooling at room temperature. However, a more practical choice is to neutralize stresses on the joint bar top and bottom [2].

4. Fatigue Analysis Overview

Most joint bars fail due to fatigue. Generally, fatigue-related cracks initiate from the top and bottom at the longitudinal center of the joint bars (Figure 18). This is where the service load-induced stresses are the highest. Joint bars have been installed and removed many times during the service life of the rail, making it difficult to determine a precise joint bar fatigue life. Joint bar fatigue life has primarily been estimated in the past using theoretical material properties and load values. However, under this research, real time load and experimental material data was used to estimate fatigue life.

Figure 18. Typical Fatigue Crack in the Bottom of the Joint Bar

4.1 Material Properties of Joint Bars Steel

The chemical composition used for making most of the joint bars is similar to American Iron and Steel Institute (AISI) 1045 steel. This material is quenched to increase the material properties

and to refine the microstructure. As Section 3.1 stated, some joint bars are also manufactured with microalloy steel. For this fatigue study, only AISI 1045 steel (quenched) and 4140 steel (quenched and tempered) were used. 4140 steel is currently not used for joint bar manufacturing, but it was studied as a possible alternate to current materials. Table 2 shows the chemical composition and test data for 1045 steel and 4140 steel. Both materials conform to current minimum AREMA requirements.

Table 2. Joint Bar Mechanical Properties and Chemical Composition

	1045 Steel (Quenched)	**4140 Steel (Quenched and Tempered)**
Carbon	0.35-0.6	0.38-0.43
Manganese	1.20 max	0.75-1.00
Phosphorus	0.07 max	0.03 max
Sulfur	0.05 max	0.04 max
Silicon		0.15-0.30
Chromium		0.80-1.10
Molybdenum		0.15-0.25
Yield Strength (ksi)	85 ksi	145 ksi
Tensile Strength (ksi)	135 ksi	160 ksi
Elongation	14%	15%
Reduction of Area	33%	49%
Charpy (ft-lb) at 32 °F	15 ft-lb	24 ft-lb

4.2 Microstructure of Joint Bar Steel Materials

The microstructure of the current standard joint bar material is ferrite (light etching) plus pearlite (dark etching) [1]. Figure 19 (left) shows the surface is decarburized, indicated with dark etching at the surface. The depth of decarburization is within the limit recommended by AREMA. However, in general, decarburization can reduce the fatigue strength of material significantly.

The most important observation of the microstructure examination was the amount of surface discontinuities and cracks in the 1045 steel. Regardless of the mechanical properties of the steel, a bar containing surface cracking of this nature would be prone to failure due to fatigue. The cracks create sharp stress risers, which are probable fatigue initiation points. The combination of surface cracks and the reduced strength of the material due to decarburization increase the likelihood of fatigue initiation. These cracks most likely occur from the quenching processes.

Comparatively, 4140 steel has a tempered martensite structure, which may have better fatigue strength than the ferrite plus pearlite microstructure of 1045 steel. Figure 19 (right) shows no decarburization on the surface of 4140 steel. In addition, the microstructure was the same throughout the cross section.

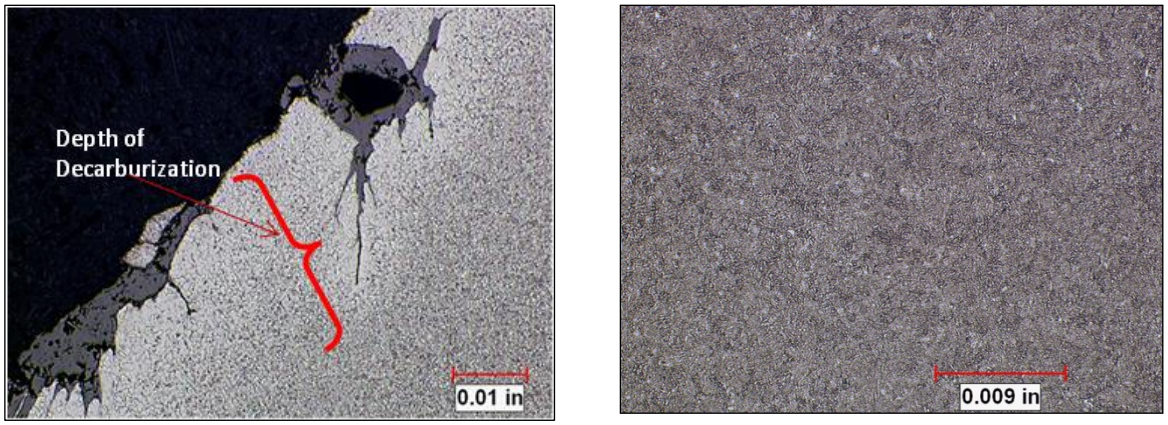

Figure 19. (Left) 1045 Steel, (Right) 4140 Steel Microstructures

4.3 Load Environment

Joint bars experience maximum tensile strains in the bottom edge of the longitudinal center and maximum compressive strains in the top edge of the longitudinal center. Strain levels vary throughout the service life of joint bars because of variations in foundation conditions. Dynamic bending strains on the top and bottom of joint bars were measured under the FAST train, which had 315,000-pound cars at various tonnage levels. The dynamic strain data was then converted into stress environment histograms. These histograms were used in the fatigue analysis. Load environment was discussed in detail in a previous report [3] and in Section 2 of this report.

4.4 Development of Stress and Strain Fatigue Life Curves

Fatigue testing to prepare S-N curves was conducted on both current and proposed candidate materials by a third-party test laboratory. Current joint bar material composition is similar to that of 1045 steel, which was quenched to further improve the material properties. Candidate material has a composition similar to that of 4140 steel, which was quenched and tempered to improve the mechanical properties.

High cycle fatigue and low cycle fatigue testing followed the standard procedures of American Society of Testing Materials (ASTM) E606-04 and ASTM E466-07, respectively.

4.4.1 High Cycle Fatigue Testing

Fifteen samples of 4140 steel and two samples of 1045 steel were tested up to 10 million cycles using a sinusoidal wave at a frequency of 1 Hz and R-ratio of 0. Figure 20 shows the stress and cycle levels applied on each sample. Multiple samples were tested at the same stress and cycle levels. Therefore, data points shown on the graph are lower than the number of samples. Just one sample failed prematurely at 58,000 cycles. One sample accumulated 15 million cycles without failure. All other samples did not fail after 10 million cycles; therefore, high cycle fatigue testing was discontinued.

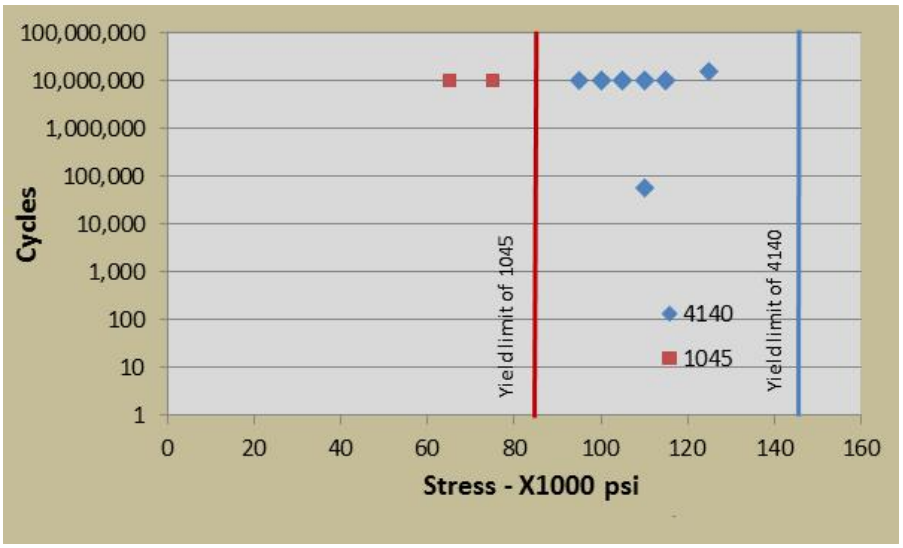

Figure 20. Results of High Cycle Fatigue Testing

4.4.2 Low Cycle Fatigue Testing

Five samples of 1045 steel were tested at strain levels of 0.5, 0.6, 0.7, 0.8 and 0.9 percent. Three samples tested at a strain level of less than 0.5 percent did not fail after 2 million cycles. Five samples of 4140 steel were also tested at strain levels of 0.5, 0.6, 0.7, 0.8 and 0.9 percent. Four samples tested at a strain level of 0.45 percent and below did not fail after 2 million cycles. Failure criteria for both materials were defined as the point where the maximum stress decreased to 50 percent of the stabilized maximum stress. The specimens were tested at room temperature using a triangular waveform at a frequency of 1 Hz, and an R-ratio of 0.

Mean was calculated for only three data points, disregarding the lowest and highest data point at each strain level. Mean minus two standard deviations was then calculated at each level, which provides a 93 percent survival rate.

After the specimen “mean minus two standard deviations” strain-life curves were established, the size, load type, and surface finish factors were applied to acquire the component life curve. This was done by modifying only the elastic portion of the curve for load type, size, and surface finish effects.

The strain and stress range at 2.0E6 cycles was reduced by a factor determined by size, load type, and surface finish effects. Different literature references revealed significantly different values for some of the reduction factors. As a result, the life prediction is a range rather than a single point value.

Factors are as follows:

4140 steel	Size effects = 1.0
	Load effects = 1.0
	Surface effects = 0.42
1045 steel	Size effects = 1.0
	Load effects = 1.0
	Surface effects = 0.47

Figure 21 shows the S-N curves for 4140 steel (top) and 1045 steel (bottom).

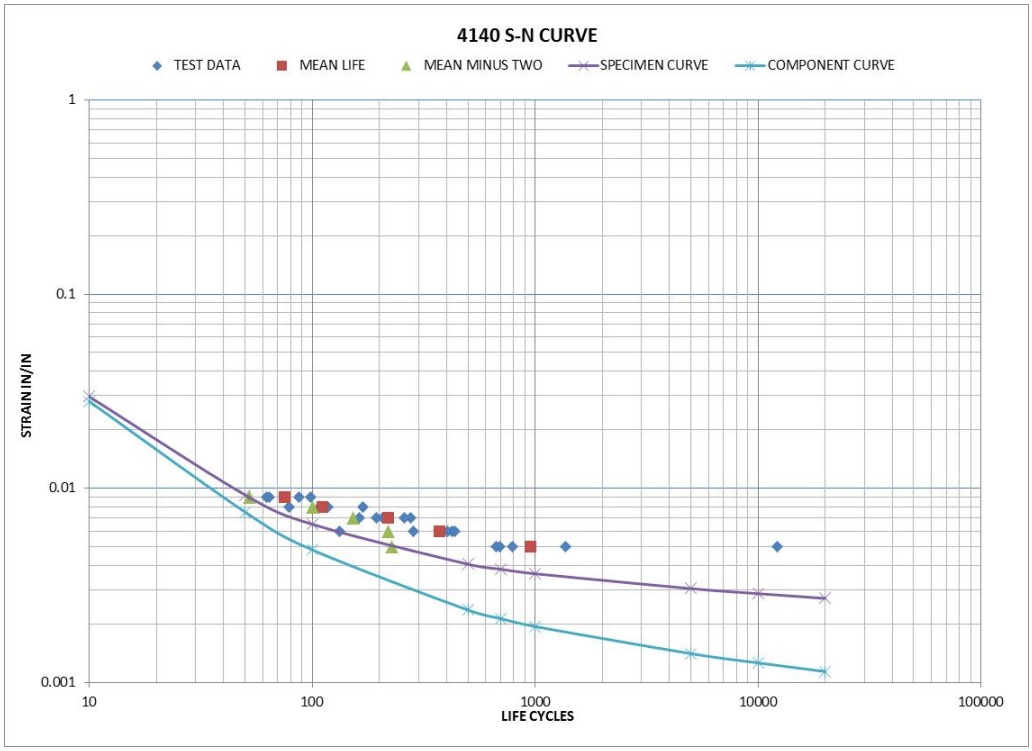

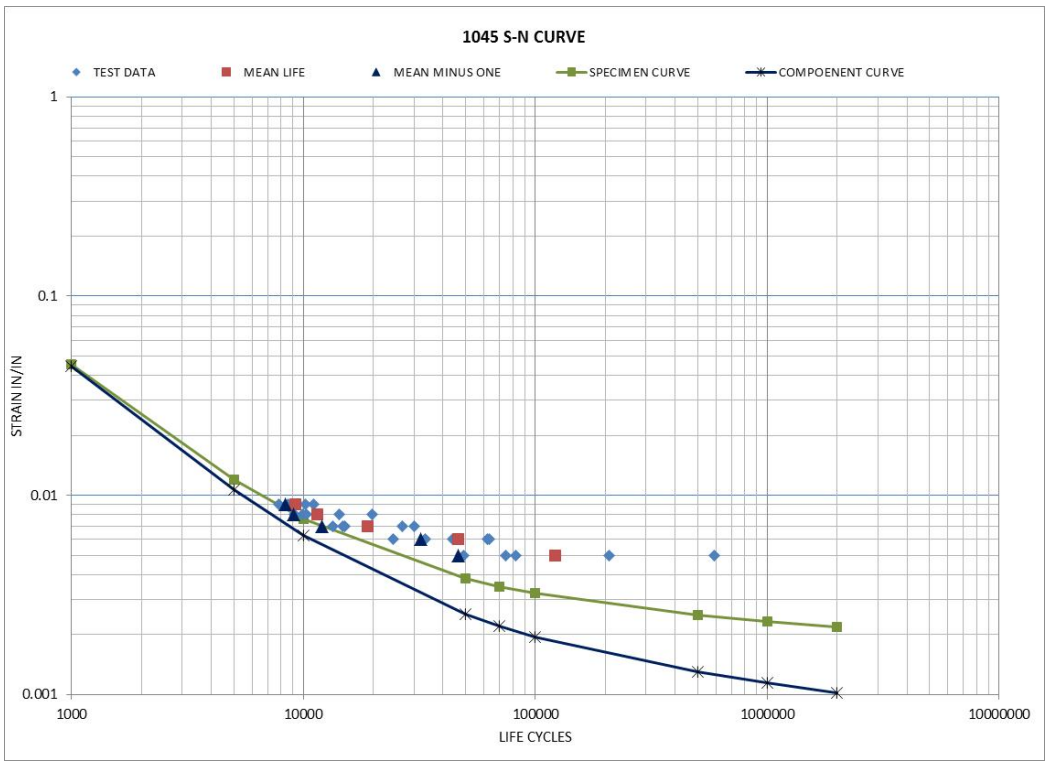

Figure 21. (Top) 4140 Steel, (Bottom) 1045 Steel Strain-Life Curves

4.5 Fatigue Analysis

The fatigue life prediction software, nCode Glyphworks, was used to perform the cumulative damage strain-life analysis. The software calculates damage for each cycle contained in the stress and strain environment. Minor's cumulative damage techniques are used to calculate damage for every cycle in the stress environment. The following assumptions, in conjunction with the total strain-life curve properties, were used to produce fatigue life predictions with the nCode software:

- Any stress and strain range corresponding to a life greater than 1.0E8 cycles on the strain-life curve did not cause any damage. The result is that some fatigue damage can be accumulated even at relatively low strain range values.
- Smith-Watson-Topper damage model was used to account for mean stress values not equal to zero during each cycle [4]. The bending strain history obtained from a previous study was used as input for analysis [3]. Similarly, the material properties (S-N curves) developed during the current study were used as material input. Fatigue life was calculated in train passes and then changed to MGT.

Results from the strain-life analysis are summarized in the following section.

4.6 Discussion and Conclusions

Figure 22 shows fatigue life calculated for three types of joint bars—6-hole joint bars, 8-hole joint bars, and 6-hole insulated joint bars. Although the minimum of 450 MGT life was calculated, the bulk of the data shows life of more than 1,100 MGT. For standard joint bars, 6-hole and 8-hole, average life of approximately 10,000 MGT was calculated. Fatigue life of insulated joint bars was even higher. Considering current traffic levels, this is essentially an unlimited fatigue life. Experimental results of high cycle fatigue as shown in Figure 20 also predict that the fatigue life of current joint bar material is fairly high. Both the experimental and analytical calculations assumed that material surfaces were free of any stress risers.

The joint bar fatigue failures seen in service are likely due to surface material discontinuities created as a result of manufacturing processes and mechanical notches induced during handling. Another factor that potentially affects the fatigue life is deteriorated foundations under rail joints.

Generally, an increase in yield strength may result in lower toughness and/or lower fatigue life [1]. Section 4.1 showed that 4140 steel has a 76 percent higher yield strength than 1045 steel. Table 2 also shows that Charpy test values, which are a measure of toughness, were also higher for 4140 steel. However, S-N curves for low cycle fatigue show that fatigue life is similar for 4140 steel and 1045 steel. It may be concluded that increasing the mechanical strength of joint bar material is not likely to affect the fatigue life of joint bars.

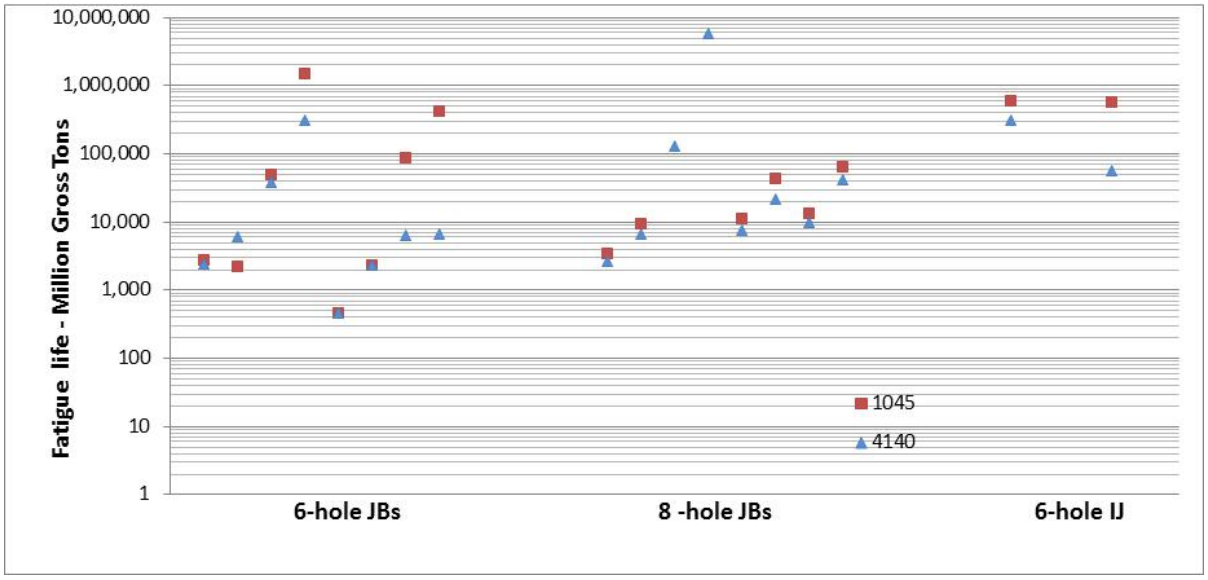

Figure 22. Fatigue Life of Joint Bar Materials

5. References

1. Akhtar, M.N., Davis, D.D., Guzel, H. March 2012. "Improved Joint Bar Service Life – Manufacturing Processes and Materials." *Technology Digest* TD-12-006, Association of American Railroads, Transportation Technology Center, Inc., Pueblo, CO.
2. Akhtar, M.N., Davis, D.D. May 2011. "Residual Stress Management of Rail Joint Bars." *Technology Digest* TD 11-016, Association of American Railroads, Transportation Technology Center, Inc., Pueblo, CO.
3. Akhtar, M. and Davis, D. April 2013. "Load Environment of Rail Joint Bars – Phase I, Effects of Track Parameters on Stresses and Crack Growth." DOT/FRA/ORD-13/24, Federal Railroad Administration, Washington, DC.
4. Socie, D., Sharma, V. December 1990. "Strain Life Method for Fatigue Analysis of Freight Cars and Components." Research R-report R-762, Association of American Railroads, Washington, DC.

Abbreviations and Acronyms

AAR	Association of American Railroads
AISI	American Iron and Steel Institute
AREMA	American Railway Engineering and Maintenance-of-Way Association
ASTM	American Society of Testing Materials
FAST	Facility for Accelerated Service Testing
FRA	Federal Railroad Administration
ksi	thousand pounds per square inch
lb	pound
mph	miles per hour
MGT	million gross tons
psi	pounds per square inch
TTCI	Transportation Technology Center, Inc. (the company)
UTS	ultimate tensile strength